Imaging Modalities and Differential Diagnosis

3

Matthew T. Houdek and Benjamin M. Howe

3.1 Introduction

The pelvis is a common site for primary and metastatic tumors. Although common, the diagnosis can be difficult. Patients with pelvic tumors often have a variable and nonspecific clinical presentation, with symptoms ranging from pain, fever, fatigue, bowel/bladder changes, weight loss, and lower extremity swelling. Due to the heterogeneity in the presentation, the diagnosis may be delayed until the tumors are either large enough to cause significant symptoms or pathologic fracture, or they are incidentally found on imaging for nonspecific symptoms such as back or hip pain. In the workup of a pelvic mass, plain radiographs, computed tomography (CT), magnetic resonance imaging (MRI), and positron emission tomography/computed tomography (PET/CT) are used to detect and characterize these lesions. The purpose of this chapter is to review the use of these imaging modalities and define the characteristics of some of the common lesions of the pelvis.

3.2 Imaging Modalities

3.2.1 Plain Radiographs

Plain radiographs are commonly the initial study in the evaluation of pelvic tumors. Large soft tissues masses may displace the bowel gas, obscure normal fat planes, or distort interfaces between muscle and the overlying fat allowing for detection on plain radiographs. Even very large soft tissue tumors can be challenging to detect on plain radiographs given the overlying bowel gas and soft tissues.

M. T. Houdek (✉)
Department of Orthopedic Surgery, Mayo Clinic, Rochester, MN, USA
e-mail: Houdek.Matthew@mayo.edu

B. M. Howe
Department of Radiology, Mayo Clinic, Rochester, MN, USA

The overlying soft tissues and bowel gas and complex osseous anatomy of the pelvis limit the detection of pelvic bone tumors on plain radiographs. Initial radiographs in unsuspected pelvic bone tumors are typically anterior-posterior projection, and the lack of orthogonal imaging limits the confident detection of pelvic bone tumors on the initial radiographs (Fig. 3.1). Likewise, the thick cancellous bone of the ilium allows bone tumors to be overlooked until large and destructive. This is in contrast to lesions of the pubis and the ischium, where the thin cancellous bone and lack of overlying structures make the lesions more conspicuous.

After detection of an osseous lesion on plain radiographs, an attempt should be made to categorize a lesion as having either nonaggressive or aggressive features. This distinction is more challenging in the pelvis compared to tumors of the extremities given the technical limitations of pelvic radiographs discussed above. The three categories of bone destruction are purely lytic, purely sclerotic, and mixed lytic and sclerotic.

The patterns of bone destruction and reaction of the host bone aid in the determination of aggressive and nonaggressive of lytic bone lesions. The margin formed between the lytic lesions and the adjacent host bone infers the aggressiveness of the tumor. In general, a narrow transition zone between the tumor and the host bone indicates a slow pattern of growth. A narrow zone of transition can be further subdivided into sclerotic and non-sclerotic. Aggressive tumors typically present with more indistinct margins (also referred to as a wide zone of transition) between the tumor and the adjacent host bone.

Periosteal reaction indicates the aggressiveness of both lytic and sclerotic bone tumors that involve or are adjacent to the cortex. The periosteal reaction type is an indicator of the host bone response and growth rate of bone lesions. Solid and unilamellar suggest an indolent growth pattern or reactive formation associated with adjacent inflammatory changes. Aggressive patterns of periosteal reaction include multi-lamellated, spiculated (also referred to as hair on end

W. Guo et al. (eds.), *Surgery of the Pelvic and Sacral Tumor*, https://doi.org/10.1007/978-94-024-1945-0_3

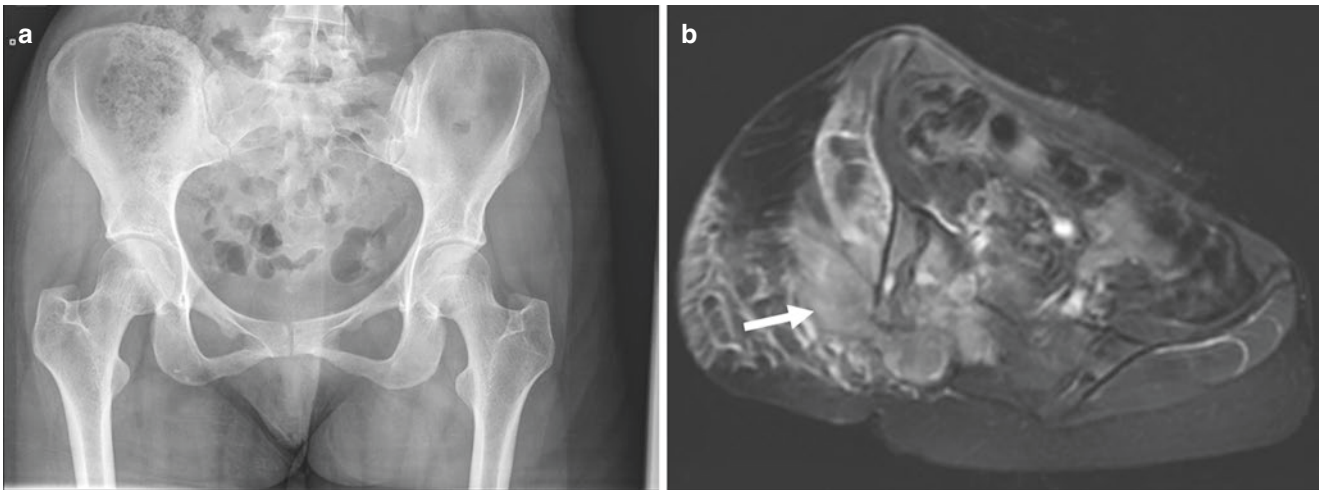

Fig. 3.1 Frontal radiograph of the pelvis (**a**) highlights the limitations of plain radiographs in the diagnosis of pelvic tumors. A subsequent axial T2-weighted fat-saturated image of the pelvis (**b**) performed 2 weeks later demonstrates a massive left sacropelvic destructive mass with marked surrounding edema and a large soft tissue mass (**b**—arrow). Biopsy demonstrated Ewing sarcoma

or sunburst), or interrupted which may present with elevation of the adjacent periosteum (Codman's triangle).

Matrix mineralization refers to calcification that forms typical patterns on the acellular matrix. The presence of either chondroid or osteoid matrix is an indicator of the type of tumor present, but matrix formation can be found in benign or malignant lesions. Chondroid matrix is defined as having a stippled, comma, or popcorn-shaped calcification (Fig. 3.2), while osteoid matrix is fluffy and ill-defined calcification.

3.2.2 Computed Tomography

CT serves as extension of radiographic evaluation of pelvic bone tumors given the limitations of plain radiographs in the detection and characterization of pelvic bone lesions. CT may better define periosteal reaction, lesions margination, and matrix formation (Fig. 3.3). CT is superior to MRI for characterizing periosteal reaction, cortical destruction, and tumor matrix formation [1]. Likewise, CT allows for the creation of three-dimensional (3D) models which can assist in the preoperative planning and assisting of surgical resection through navigated resections [2, 3]. CT is the modality of choice for image-guided percutaneous biopsy of pelvic tumors as it allows for planning a safe approach for the biopsy and documentation of the path of the needle that allows for resection of the tract in malignant tumors. Computed tomography (CT) scans are helpful in the staging of patients with pelvic sarcomas (chest, abdomen, and pelvis) and are also useful in providing cross-sectional imaging for patients with MRI contraindications.

3.2.3 Magnetic Resonance Imaging

Magnetic resonance imaging (MRI) is the modality of choice to diagnose and characterize tumors of the pelvis and has proven superior to other imaging modalities for assessing articular extension [4, 5]. Ideally performed prior to any biopsy in order to reduce the biopsy-related changes, multiple planes (axial, sagittal, and coronal) and sequences types are used to characterize the tumors and for planning resection and reconstruction. All MRI protocols for pelvic tumors should include T1-weighted non-fat-saturated and fluid-sensitive sequences (T2-weighted fat-saturated or inversion recovery). Straight axial and sagittal images are standard and should be performed in the preoperative evaluation of all pelvic tumors. Coronal images may be performed in relation to the axis of the body, which are particularly helpful in determining the extent of periacetabular tumors. Coronal oblique images orientated to the sacrum are helpful in the evaluation of lumbosacral plexus involvement. Intravenous gadolinium contrast helps distinguish cystic/necrotic versus solid components of tumors (Fig. 3.4) which may be helpful in subsequent planning of percutaneous image-guided biopsy. Fat saturation of the post-gadolinium images increases the conspicuity of the margins of the mass and allows for better visualization of the blood vessels for surgical planning. Despite the superb soft tissue contrast and ability of MRI to confidently identify the composition of multiple tissue types, many bone and soft tissue tumors cannot be confidently diagnosed on imaging alone. These lesions are referred to as indeterminate and biopsy is required for diagnosis. All MRI exams should be interpreted with plain radiographs when possible. Tumor matrix calcifications are better defined on CT and plain radiographs. Chondroid matrix has high T2 signals with a lobular

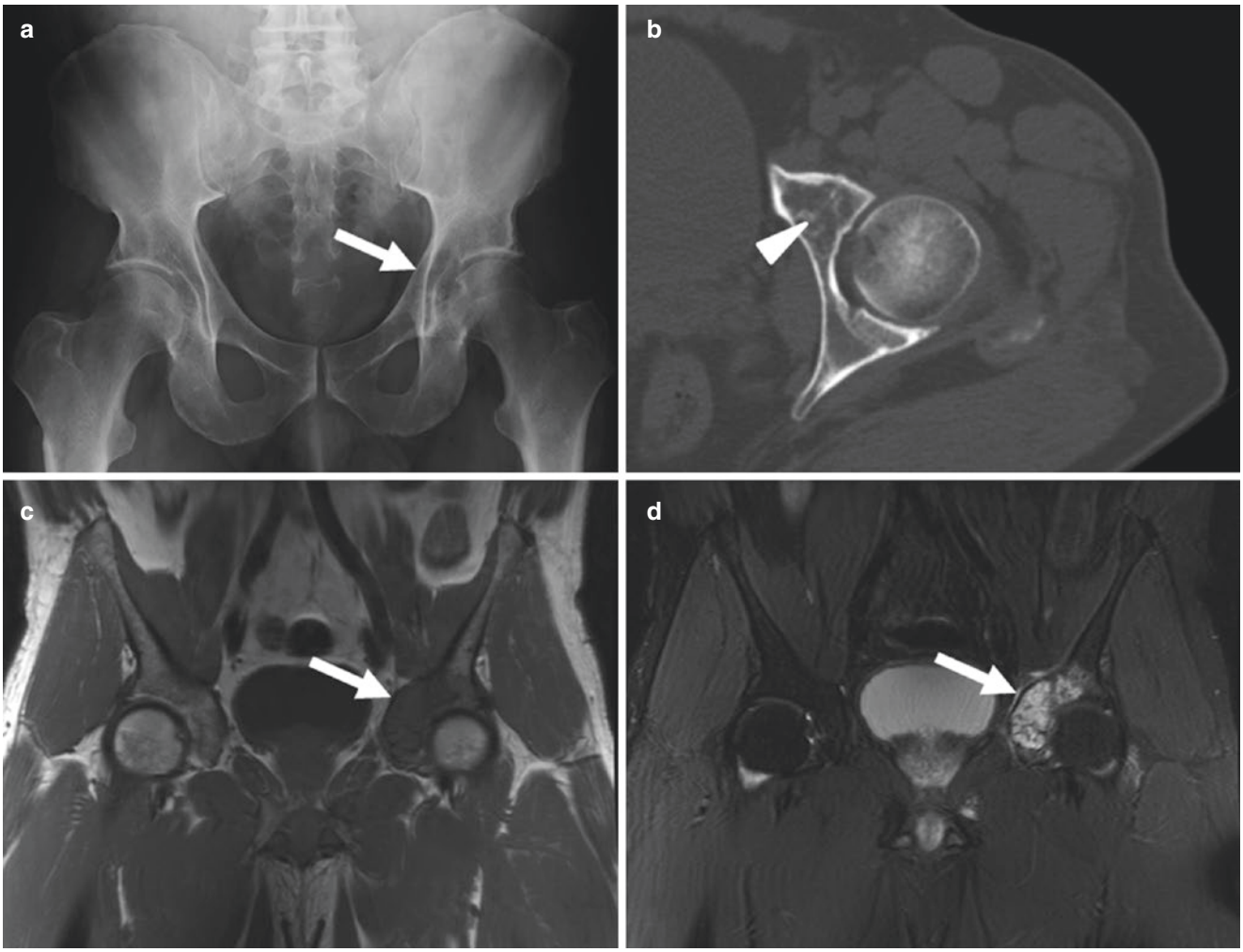

Fig. 3.2 A frontal radiograph in a 52-year-old man with left hip pain demonstrates a periacetabular lytic lesion (**a**—arrow) without cortical destruction or matrix mineralization identified. A subsequent CT demonstrates internal chondroid matrix (**b**—arrowhead). The T1 (**c**) and T2-weighted (**d**) coronal MRI images demonstrate the marrow-replacing mass with T2-weighted hyperintensity and lobulated margins consistent with a cartilage tumor. Pathology confirmed a grade II chondrosarcoma

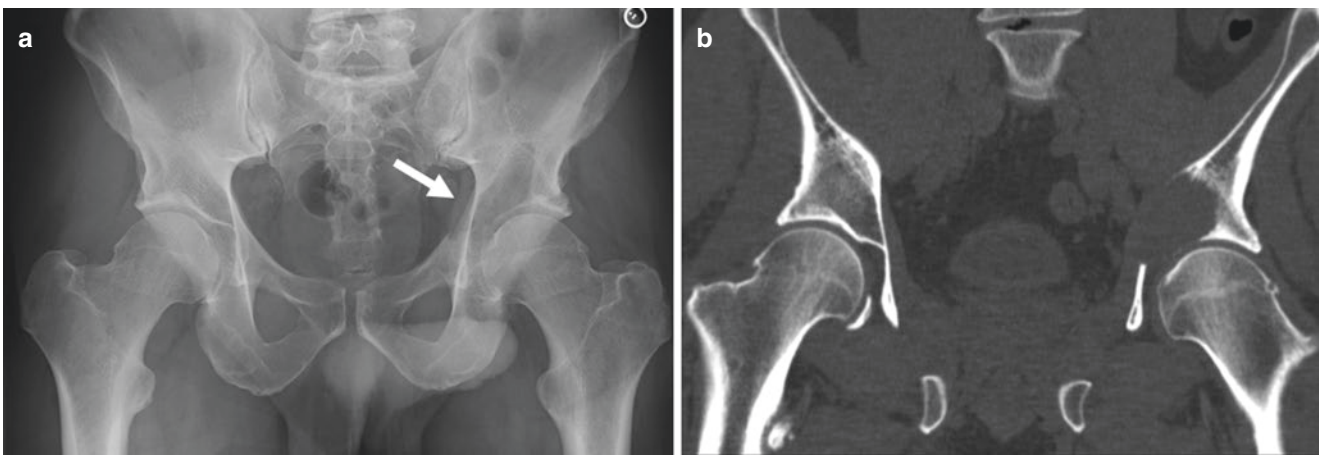

Fig. 3.3 A frontal radiograph (**a**) of a 52-year-old man demonstrates a purely lytic left periacetabular lesion. Although portions of the lesion appear to have a narrow zone of transition, cortical destruction is noted medial (**a**—arrow). A coronal CT image (**b**) of the pelvis better demonstrates the finding in this plasmacytoma

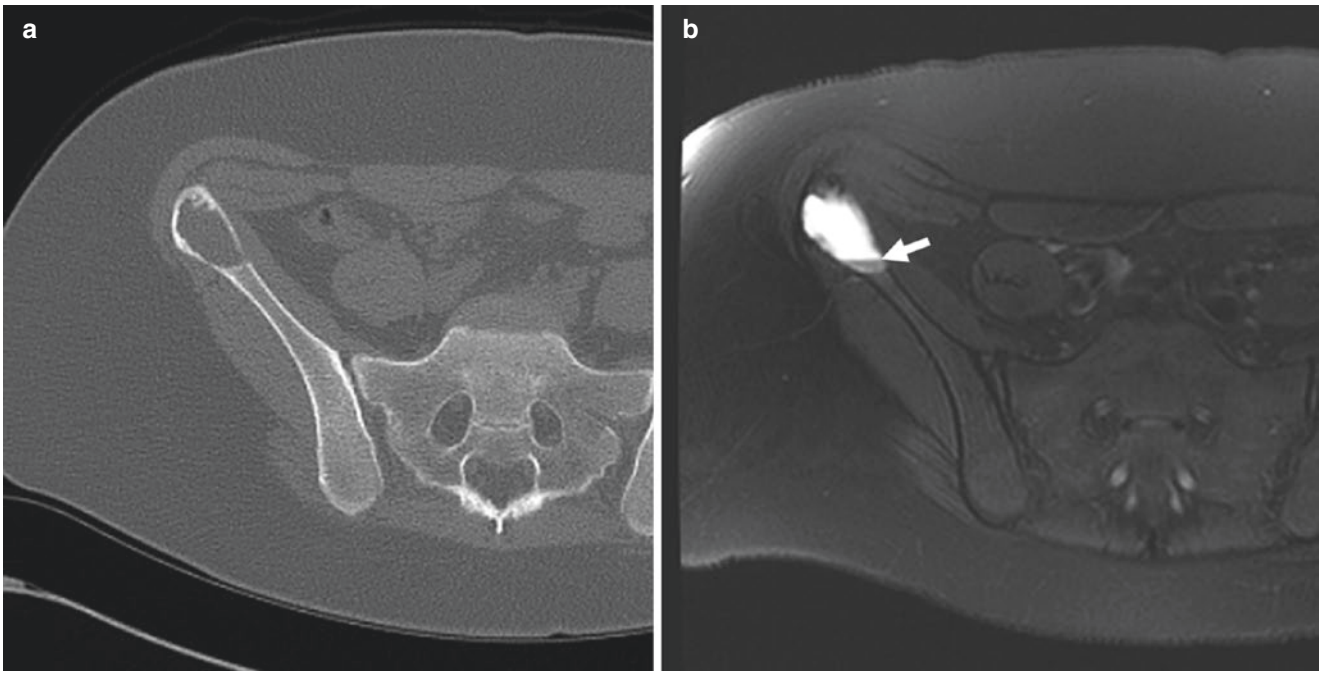

Fig. 3.4 Axial CT of the pelvis (**a**) demonstrates purely lytic lesion in the right iliac wing. The lesion has a narrow zone of transition, no cortical destruction, no periosteal reaction, and no soft tissue mass. Subsequent axial T2-weighted fat-saturated images of the pelvis show the lesion to be very hyperintense, similar to simple fluid. A linear fluid-fluid level is noted confirming the cystic nature (**b**—arrow). This lesion has benign imaging features. Curettage confirmed a simple bone cyst

growth pattern with low-signal septations (Fig. 3.2). Osteoid matrix has intermediate to low signal intensity on all sequences. The margin characterizations of lytic bone lesions used in plain radiography and CT should not be applied to MRI images. The bone tumor margins on MRI are formed by the interface of the tumor and the bone marrow which is predominantly fat in older individuals (Fig. 3.5). Aggressive intramedullary tumors may form a sharp boundary with the adjacent fatty marrow, but this does not necessarily indicate that the tumor is "well-circumscribed," a term that should be reserved for radiographs. Unlike plain radiographs, MRI is an excellent means to define the extent of a sarcoma but can overestimate the size of the tumor due to increased signal changes from edema. The spread of the tumor in the pelvis can provide clues as to whether a tumor is benign or malignant, with spread across the sacroiliac (SI) joint or articular involvement and breakthrough in the hip suggestive of a malignant process. Likewise, MRI can evaluate the extent of neurovascular involvement, specifically the T1-weighted sequences where fat planes are readily demonstrated.

In addition to being the imaging modality of choice to diagnose and characterize tumors of the pelvis, MRI is also the preferred modality to identify a preserved fat plane between the tumor and vascular structures. This is best seen in the non-fat-saturated T1 images, but it is also helpful to have post gadolinium-enhanced sequences to compare to. Although a CT angiography has better spatial resolution and is a better modality in determining patency of small arteries and intraluminal extension, it lacks the soft tissue contrast of MRI, and therefore it is difficult to determine if the vessels are abutted by the tumor. Due to this feature, MRI alone is typically adequate to determine vascular involvement.

Pre- and post-adjuvant treatment MRIs are essential for surgical planning. Often, the peritumoral edema on pretreatment studies is gone on the posttreatment studies. Typically, we plan to resect a margin beyond the pretreatment peritumoral edema in order to obtain a negative margin. This also highlights the importance of obtaining the same imaging sequences, in the same planes, for preoperative planning. Likewise, MRI imaging is also commonly used in the follow-up setting in order to evaluate for disease recurrence.

In addition to the common sequences obtained with imaging of the pelvis, specific sequences can be added in order to determine certain tumor characteristics. Since tumor tissue enhances with early dynamic images, dynamic-enhanced MRI may allow for the differentiation of tumor extension from reactive edema [6, 7]. Similarly, since active tumors enhance, and nonviable tumor doesn't readily enhance,

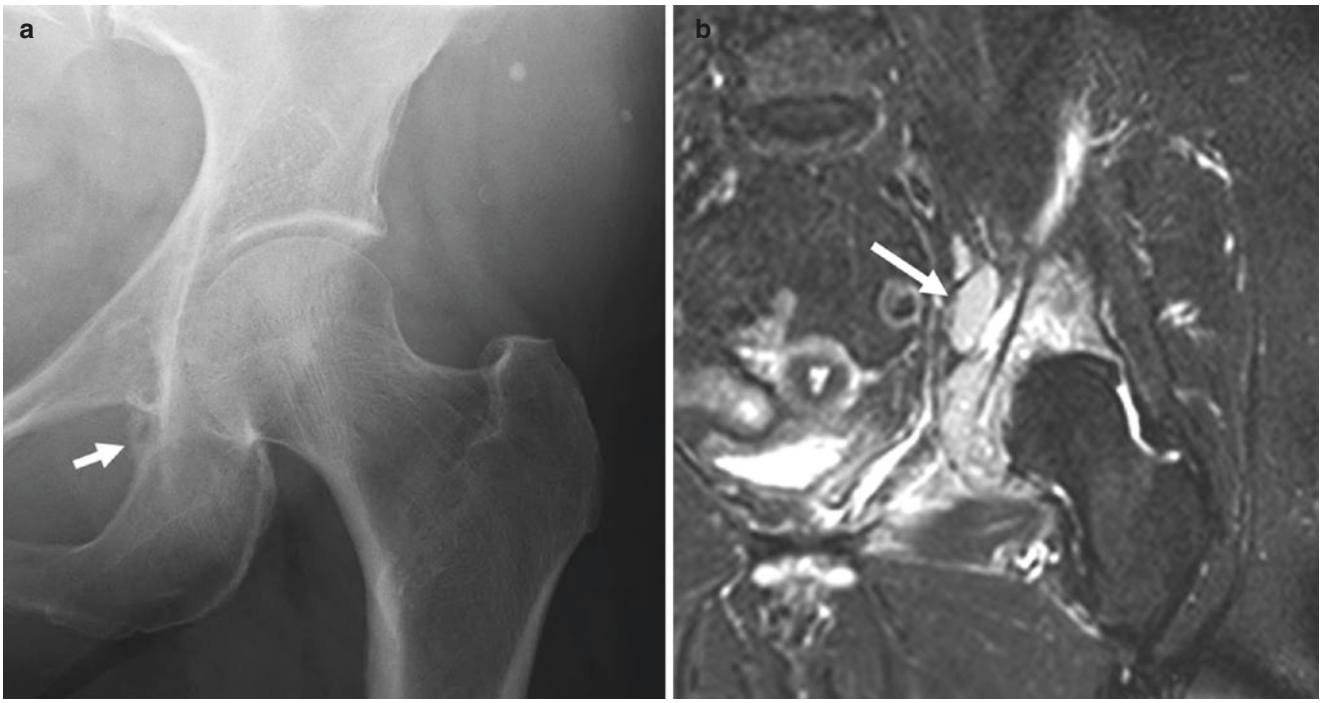

Fig. 3.5 AP radiograph of the left hip demonstrates subtle periosteal reaction along the medial margin of the ischium (**a**—arrow). The subsequent coronal STIR MR image demonstrates a large marrow-replacing mass in the left acetabulum with soft tissue extension and an enlarged left pelvic node (**b**—arrow). The differential diagnosis in the older patient is metastasis, myeloma, lymphoma, and primary sarcoma. The relative lack of findings with extensive involvement on MRI can be seen with osseous lymphoma, which was confirmed on a subsequent biopsy

dynamic MRI can assess the response to treatment by determining the extent of tumor necrosis [8].

3.2.4 Positron Emission Tomography/Computed Tomography

Positron emission tomography/computed tomography (PET/CT) has recently become increasingly used in the diagnosis and evaluation of pelvic tumors. PET/CT enhances the use of CT imaging and allows for the differentiation of benign from malignant lesions, detection of metastatic disease, and tumor surveillance [9]. PET/CT is based on the uptake of [^{18}F]-2-deoxy-2-fluoro-D-glucose (FDG) in the tumor which is associated with cellular glycolysis. The degree of FDG avidity can be compared to the metabolic activity of the surrounding tissue, with increased uptake typically found in malignant tumors [10–13]. In a study by Aoki and colleagues [13], the authors noted an increased uptake of two times greater uptake for benign lesions and four times greater uptake for malignant lesions compared to background tissue for bone lesions. The strength of PET/CT is in the ability to stage malignant tumors.

3.3 Imaging Features of Common Pelvic Tumors

3.3.1 Malignant Lesions

3.3.1.1 Chondrosarcoma

Chondrosarcoma is the most common primary malignancy of the bones of the pelvis and is characterized by a malignant proliferation of chondroid matrix. Chondrosarcoma can either be a primary bone tumor or a secondary tumor arising from an enchondroma or osteochondroma. In the pelvis, the tumors are typically low grade, with high-grade tumors having a worse prognosis [14].

Primary cartilage tumors in the pelvis should be approached with caution as the imaging features applied to differentiate enchondromas from low-grade chondrosarcomas in the extremities should not be directly applied to the pelvis. Aside from hereditary multiple enchondromatoses, pelvic enchondromas are rare. The incidence of chondrosarcoma and enchondromas is opposite from the extremities where benign enchondromas are quite common [15]. Typically, low-grade tumors have well-defined margins and may have cortical expansion. Chondroid matrix may or may

not be present in pelvic chondrosarcoma. The "rings and arcs" pattern of chondroid matrix mineralization is better delineating on CT than plain radiographs for pelvic chondrosarcomas. On CT, the matrix is often described as stippled, and there can be cortical destruction, periosteal reaction, pathologic fracture, and an associated soft tissue mass with chondrosarcomas. On MRI, the mass demonstrates lobules of high T2 signal consistent with chondroid matrix. Dedifferentiated chondrosarcoma has components of both low-grade and high-grade tumors. A large lytic destructive tumor with a soft tissue mass adjacent to a cartilage tumor with matrix mineralization suggests the diagnosis of dedifferentiated chondrosarcoma [16].

Secondary chondrosarcoma may arise in the cartilage cap of osteochondromas (Fig. 3.6). A small cap, less than 2 cm thick, is typically benign. A cartilage cap thicker than 2 cm with irregularity of the osseous stalk, irregular calcifications, and a poorly defined cap is suspicious for malignant transformation into a chondrosarcoma [17].

3.3.1.2 Osteogenic Sarcoma

Although not as common in the pelvis as the extremities, conventional osteogenic sarcoma is the second most common primary malignancy of bone [18]. In the pelvis, osteosarcoma is most commonly located in the ilium and acetabulum (Fig. 3.7). On plain radiographs, osteosarcomas have aggressive features with "cloud-like" osteoid matrix formation and mixed areas of osteolysis and sclerosis. Osteosarcomas with greater areas of osteolysis are more aggressive tumors and associated with cortical destruction and a soft tissue mass. The diagnosis of osteosarcoma can often be made on plain radiographs alone. MRI is typically used to evaluate the

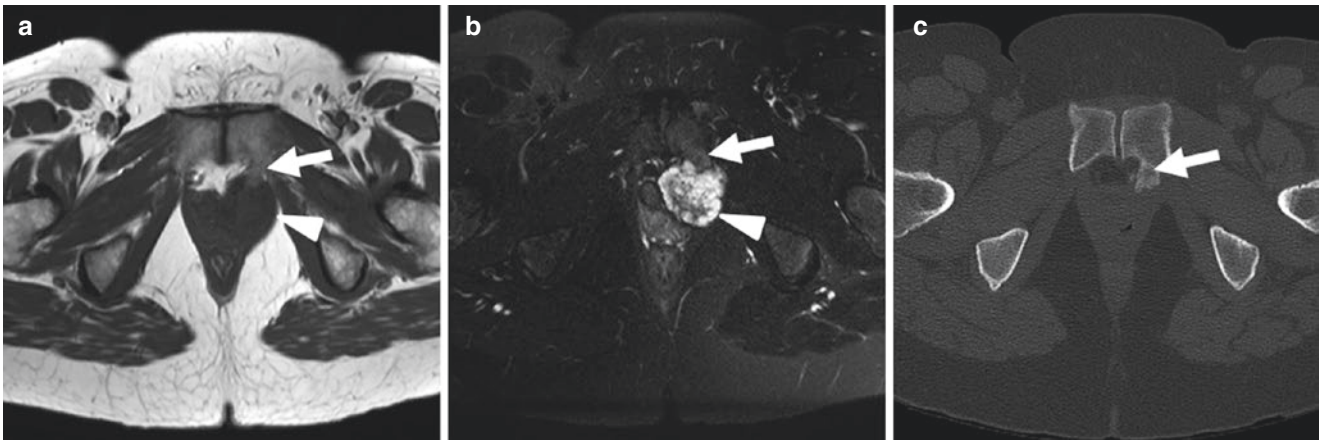

Fig. 3.6 Axial T1- (**a**) and T2-weighted fat-saturated (**b**) MR images demonstrate a lobulated T2 hyperintense mass compatible with a cartilage tumor (**a** and **b**—arrowheads). An osseous stalk from the adjacent pubic bone can be seen on the MRI (**a** and **b**—arrows) and is better visualized on the subsequent CT (**c**—arrow)

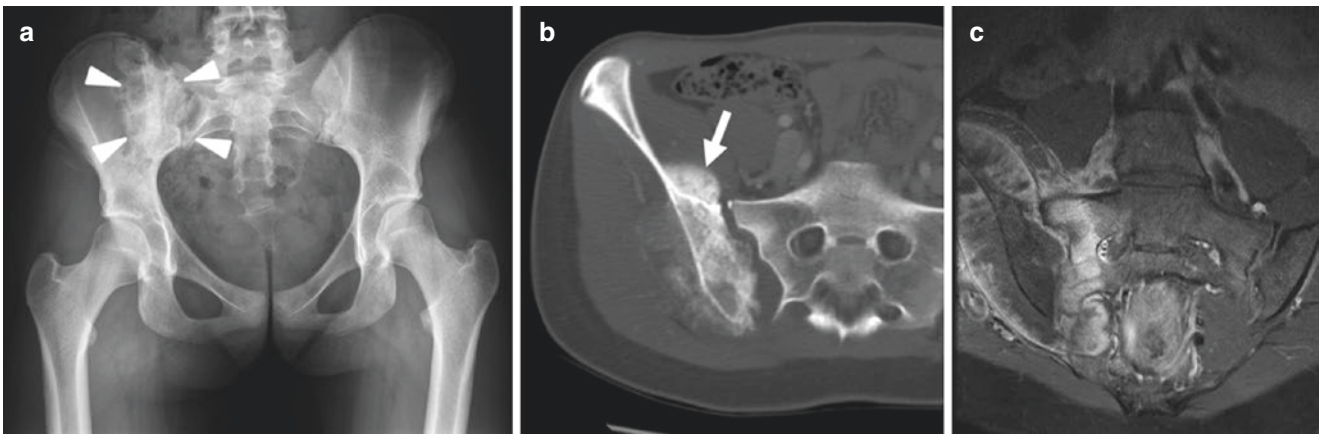

Fig. 3.7 A frontal radiograph (**a**) in a 16-year-old with low back pain demonstrates a large sclerotic lesion projecting over the sacroiliac joint (**a**—arrowheads). An axial CT image shows a large associated soft tissue mass with cloudy-like areas of matrix mineralization (**b**—arrow) diagnostic of osteoid matrix in this osteosarcoma. A coronal oblique T2-weighted fat-saturated MR image of the sacrum (**c**) shows the extent of the soft tissue mass and involvement of the sacrum

extent of the soft tissue mass and involvement of neurovascular structures. On MRI, the mass has heterogeneous signal intensity of low and high signal on T1 and T2 imaging and is the most common sarcoma with fluid-fluid levels [19]. Even with aggressive treatments, the reported 5-year overall survival of osteosarcoma of the pelvis is 38% [20].

3.3.1.3 Ewing Sarcoma

The most common axial site for Ewing sarcoma is the pelvis, and the imaging features of Ewing sarcoma of the pelvis are similar to that of the extremities [21]. On plain radiographs and CT, there is a moth-eaten and permeative destructive lesion with ill-defined cortical margins. In contrast to extremity Ewing, in the pelvis, there is often more reactive sclerosis with a concentric expansion of the cortical bone, leading to the classic "onion-skin" appearance. On MRI, the tumor is hypo- or isointense on T1, with increased signal intensity on T2 (Fig. 3.1). On MR, an associated soft tissue mass is commonly seen, most frequently in the gluteal and iliac compartments [22]. Likewise, Ewing sarcoma can cross the SI joint and is associated with a 75% 5-year survival with appropriate treatment [23].

3.3.1.4 Chordoma

Chordomas are the most common malignant lesions of the sacrum [24]. Since they are typically slow-growing tumors, they are frequently quite large at the time of diagnosis. On radiographs, chordomas appear as a solitary, midline lytic lesion centered typically at the lower sacral vertebrae (3rd through 5th) [25]. Although not readily apparent on radiographs, there is always a soft tissue mass, and in half of the patients, it is associated with focal calcifications and epidural extension on MRI and CT [26]. On MRI (Fig. 3.8), the tumor is slightly hypointense to isointense on T1 and, due to a high concentration of mucin, hyperintense on T2-weighted signal [25]. Having an adequate surgical margin has been found to be the most important factor on local disease recurrence and overall survival [27].

3.3.1.5 Liposarcoma

Liposarcomas are common tumors of the retroperitoneum [28, 29]. In the extremities, the term well-differentiated liposarcoma has been replaced by atypical lipomatous tumors given they do not metastasize unless they are dedifferentiated. In the pelvis, this may lead to confusion in the evaluation of greater sciatic notch tumors (Fig. 3.9). The MR features differentiating lipomas from atypical lipomatous tumors in the extremities have been well described. Typically, atypical lipomatous tumors of the extremities will have at least 75% adipose tissue; however, tumors with as little as 25% adipose tissue have been reported [30]. The use of contrast is helpful in differentiating between a benign lipoma and a well-differentiated liposarcoma. In a lipoma, the septations are thin (<2 mm thick) and have a faint enhancement; however, in a liposarcoma, they are thick and enhance on fat-suppressed T1 images [31]. In contrast, dedifferentiated liposarcomas have a non-lipomatous soft tissue mass, often with areas of necrosis and hemorrhage [32]. A biopsy should be considered for any solid, enhancing non-lipomatous mass associated with a lipomatous tumor to exclude tumor dedifferentiation. Notable benign mimickers of pelvic liposarcoma are extramedullary hematopoiesis and extra-adrenal myelolipoma. Both of these benign masses can occur in the presacral space and contain both lipomatous and soft tissue elements. Biopsy is typically necessary to confirm the diagnosis and to exclude liposarcoma.

Since they are fatty tumors, sometimes, they may be apparent on plain radiographs; however, the utility of plain

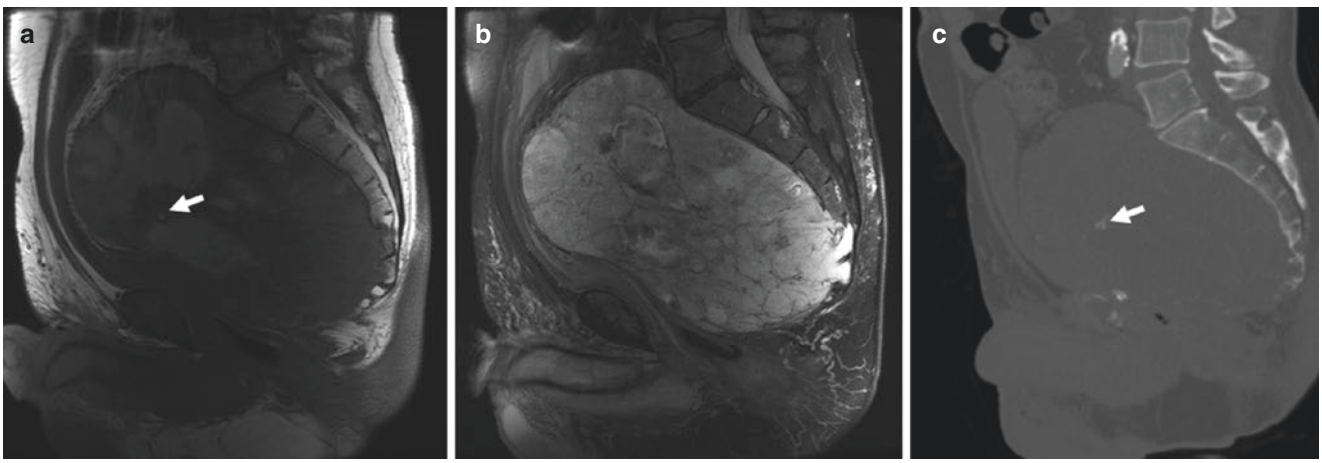

Fig. 3.8 Sagittal T1 (**a**) MR image demonstrating slightly hypointense mass with areas of increased signal intensity consistent with hemorrhage arising from the coccyx and S5 vertebrae. Sagittal T2-weighted (**b**) MR image demonstrates a lobulated T2 hyperintense mass with areas of septation and also focal calcifications (arrows) which are readily apparent on CT (**c**). Biopsy was consistent with a chordoma

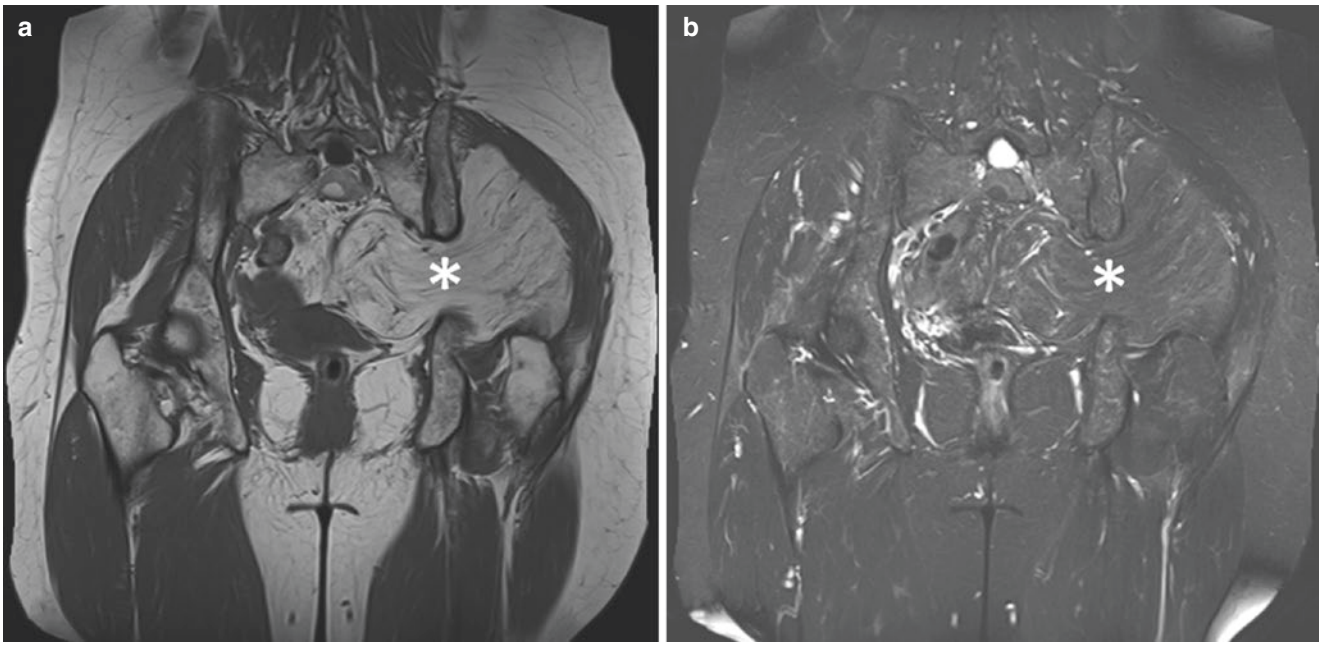

Fig. 3.9 Coronal T1- (**a**) and T2-weighted (**b**) images of the pelvis demonstrate a large "dumbbell-shaped" mass in the left greater sciatic notch (**a** and **b**—asterisks). The mass has both intrapelvic and extrapelvic involvement. The mass is comprised almost entirely of mature fat, following the signal characteristics of the subcutaneous fat compatible with a lipomatous tumor. The size, location, and internal septations raise concern for well-differentiated liposarcoma versus a large benign lipoma

radiographs for diagnosing these tumors is limited. On MRI, a well-differentiated liposarcoma images as predominantly fatty mass (hyperintense on T1, hypointense on T2), however, will have decreased signal intensity T1 in the areas of the thickened tumor septation and nodular areas [30].

3.3.1.6 Metastatic Disease

Metastatic disease is the most common malignant tumor of the pelvis and sacrum and, along with metastasis and myeloma, should be considered in the differential diagnosis of aggressive pelvic bone lesions in adults. Osseous metastatic disease may be lytic, sclerotic, or mixed lytic and sclerotic. Since solitary metastatic lesion can be treated and potentially cured with an en bloc resection, staging studies are recommended to exclude any additional sites of metastatic disease. Lytic lesions can be difficult to identify on plain radiographs; however, they are readily apparent on MRI due to confluent replacement of the fatty marrow on T1-weighted sequences and increase signal on fluid-sensitive sequences.

3.3.2 Benign Lesions

3.3.2.1 Giant Cell Tumor

Although classified as a benign lesion, giant cell tumors (GCT) are locally aggressive tumors with the ability to metastasize to the lungs [25]. In the extremities, they are metaphyseal and extend into the epiphysis. They most commonly involve the sacrum in the pelvis. On radiographs, GCT are lytic, often with a soft tissue mass (Fig. 3.10). GCTs typically lack periostitis, calcifications, and osteoid formation [33]. MRI is used to assess the extent of soft tissue, intra-articular, and interosseous involvement. GCT is hypointense on T1 and has a heterogeneous T2 signal; however, the solid component of GCT is dark on T2, due to hemosiderin [33]. Although GCT has a characteristic appearance in the long bones, pelvic GCTs have less specific imaging features, and biopsy is typically required to confirm the diagnosis.

3.3.2.2 Osteochondroma

Osteochondromas are the most common benign bone tumors, and the imaging features are characteristic. They are either a broad-based, sessile growth or a pedunculated lesion growing away from the growth plate with continuity of the cortex and medullary canal. Typically, these lesions are found incidentally; however, patients can also present with a painless, nontender mass and can be symptomatic if they compress on adjacent structures. A thin cartilage cap, less than 2 cm thick, however, larger lesions with irregular calcifications and a poorly defined cap are suspicious for malignant transformation into a chondrosarcoma [17].

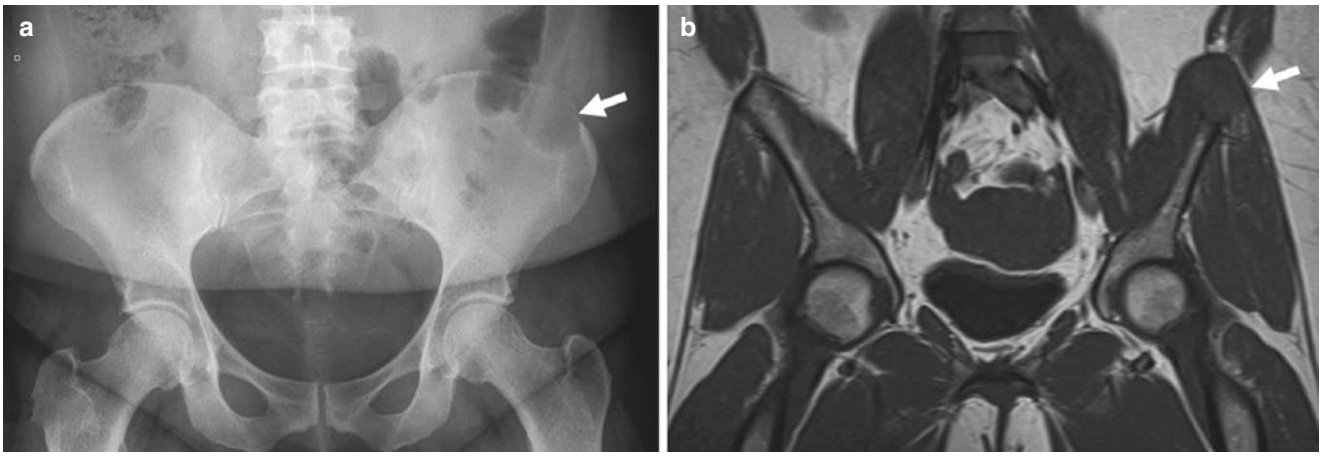

Fig. 3.10 Frontal radiograph of the pelvic demonstrates a lytic lesion in the left iliac wing with a narrow zone of transition (**a**—arrow). A subsequent coronal T1 MRI image demonstrates the expansile lytic lesion (**b**—arrow) diagnosed as a giant cell tumor on pathology

3.3.2.3 Aneurysmal Bone Cyst

An aneurysmal bone cyst (ABC) is an expansile osteolytic lesion with blood-filled spaces separated by connective tissue septa which contain bone, osteoid, and osteoclast giant cells [34]. The pelvis is a common location for these lesions in flat bones, accounting for up to 50% of cases [34]. Although the origin of an ABC is not entirely understood, they have characteristic imaging features. On plain radiographics, they are eccentric, lytic lesions with a well-circumscribed border. On CT and MRI, a cystic space with fluid-fluid levels and contrast enhancement of the septa is apparent. On MRI, there will be a high-to-low signal intensity of the fluid-fluid levels on T1- and T2-weigheted sequences. Well-circumscribed lesions on CT or radiographs that are comprised almost entirely with fluid-fluid levels on MRI are typically benign and are usually primary ABCs. Secondary ABCs can arise in a variety of other bone tumors with GCT and osteoblastomas most commonly associated with secondary ABC formation [19]. Telangiectatic osteosarcomas are often predominantly comprised of fluid-fluid levels as seen with primary ABCs; however, the differentiation of these two entities can commonly be made on plain radiographs. Primary ABCs typically have a narrow zone of transition and expand rather than destroy the overlying cortex. Telangiectatic osteosarcoma should have an aggressive radiographic appearance with a wide zone of transition, cortical destruction, and a soft tissue mass.

3.4 Summary

This chapter discusses the imaging modalities commonly used to diagnose a pelvic mass and illustrates some of the common malignant and benign tumors found in the pelvis. The differential diagnosis of a pelvic mass is broad; however, with the proper use of plain radiographs and cross-sectional imaging (CT and MRI), the diagnosis can be narrowed. However, a biopsy is typically needed to ultimately make the final diagnosis.

References

1. Tehranzadeh J, et al. Comparison of CT and MR imaging in musculoskeletal neoplasms. J Comput Assist Tomogr. 1989;13(3):466–72.
2. Cartiaux O, et al. Improved accuracy with 3D planning and patient-specific instruments during simulated pelvic bone tumor surgery. Ann Biomed Eng. 2014;42(1):205–13.
3. Sternheim A, et al. Navigated pelvic osteotomy and tumor resection: a study assessing the accuracy and reproducibility of resection planes in Sawbones and cadavers. J Bone Joint Surg Am. 2015;97(1):40–6.
4. Pettersson H, et al. Primary musculoskeletal tumors: examination with MR imaging compared with conventional modalities. Radiology. 1987;164(1):237–41.
5. Schima W, et al. Preoperative staging of osteosarcoma: efficacy of MR imaging in detecting joint involvement. AJR Am J Roentgenol. 1994;163(5):1171–5.
6. Shapeero LG, Vanel D. Imaging evaluation of the response of high-grade osteosarcoma and Ewing sarcoma to chemotherapy with emphasis on dynamic contrast-enhanced magnetic resonance imaging. Semin Musculoskelet Radiol. 2000;4(1):137–46.
7. Lang P, et al. Musculoskeletal neoplasm: perineoplastic edema versus tumor on dynamic postcontrast MR images with spatial mapping of instantaneous enhancement rates. Radiology. 1995;197(3):831–9.
8. Dyke JP, et al. Osteogenic and Ewing sarcomas: estimation of necrotic fraction during induction chemotherapy with dynamic contrast-enhanced MR imaging. Radiology. 2003;228(1):271–8.
9. Dehdashti F, et al. Benign versus malignant intraosseous lesions: discrimination by means of PET with 2-[F-18]fluoro-2-deoxy-D-glucose. Radiology. 1996;200(1):243–7.
10. Blodgett TM, Meltzer CC, Townsend DW. PET/CT: form and function. Radiology. 2007;242(2):360–85.

11. Lakkaraju A, et al. PET/CT in primary musculoskeletal tumours: a step forward. Eur Radiol. 2010;20(12):2959–72.
12. Feldman F, van Heertum R, Manos C. 18FDG PET scanning of benign and malignant musculoskeletal lesions. Skelet Radiol. 2003;32(4):201–8.
13. Aoki J, et al. FDG PET of primary benign and malignant bone tumors: standardized uptake value in 52 lesions. Radiology. 2001;219(3):774–7.
14. Pring ME, et al. Chondrosarcoma of the pelvis. A review of sixty-four cases. J Bone Joint Surg Am. 2001;83-A(11):1630–42.
15. Murphey MD, et al. Enchondroma versus chondrosarcoma in the appendicular skeleton: differentiating features. Radiographics. 1998;18(5):1213–37; quiz 1244–5.
16. Littrell LA, et al. Radiographic, CT, and MR imaging features of dedifferentiated chondrosarcomas: a retrospective review of 174 de novo cases. Radiographics. 2004;24(5):1397–409.
17. Brien EW, Mirra JM, Luck JV Jr. Benign and malignant cartilage tumors of bone and joint: their anatomic and theoretical basis with an emphasis on radiology, pathology and clinical biology. II. Juxtacortical cartilage tumors. Skelet Radiol. 1999;28(1):1–20.
18. Rosenberg ZS, et al. Osteosarcoma: subtle, rare, and misleading plain film features. AJR Am J Roentgenol. 1995;165(5):1209–14.
19. O'Donnell P, Saifuddin A. The prevalence and diagnostic significance of fluid-fluid levels in focal lesions of bone. Skelet Radiol. 2004;33(6):330–6.
20. Fuchs B, et al. Osteosarcoma of the pelvis: outcome analysis of surgical treatment. Clin Orthop Relat Res. 2009;467(2):510–8.
21. Bloem JL, Reidsma II. Bone and soft tissue tumors of hip and pelvis. Eur J Radiol. 2012;81(12):3793–801.
22. Gronemeyer SA, et al. Fat-saturated contrast-enhanced T1-weighted MRI in evaluation of osteosarcoma and Ewing sarcoma. J Magn Reson Imaging. 1997;7(3):585–9.
23. Frassica FJ, et al. Ewing sarcoma of the pelvis. Clinicopathological features and treatment. J Bone Joint Surg Am. 1993;75(10):1457–65.
24. Llauger J, et al. Primary tumors of the sacrum: diagnostic imaging. AJR Am J Roentgenol. 2000;174(2):417–24.
25. Diel J, et al. The sacrum: pathologic spectrum, multimodality imaging, and subspecialty approach. Radiographics. 2001;21(1):83–104.
26. Soo MY. Chordoma: review of clinicoradiological features and factors affecting survival. Australas Radiol. 2001;45(4):427–34.
27. Fuchs B, et al. Operative management of sacral chordoma. J Bone Joint Surg Am. 2005;87(10):2211–6.
28. Weiss SW, Rao VK. Well-differentiated liposarcoma (atypical lipoma) of deep soft tissue of the extremities, retroperitoneum, and miscellaneous sites. A follow-up study of 92 cases with analysis of the incidence of "dedifferentiation". Am J Surg Pathol. 1992;16(11):1051–8.
29. Lucas DR, et al. Well-differentiated liposarcoma. The Mayo Clinic experience with 58 cases. Am J Clin Pathol. 1994;102(5):677–83.
30. Kransdorf MJ, et al. Imaging of fatty tumors: distinction of lipoma and well-differentiated liposarcoma. Radiology. 2002;224(1):99–104.
31. Hosono M, et al. Septum-like structures in lipoma and liposarcoma: MR imaging and pathologic correlation. Skelet Radiol. 1997;26(3):150–4.
32. Kransdorf MJ, Meis JM, Jelinek JS. Dedifferentiated liposarcoma of the extremities: imaging findings in four patients. AJR Am J Roentgenol. 1993;161(1):127–30.
33. Murphey MD, et al. From the archives of AFIP. Imaging of giant cell tumor and giant cell reparative granuloma of bone: radiologic-pathologic correlation. Radiographics. 2001;21(5):1283–309.
34. Vergel De Dios AM, et al. Aneurysmal bone cyst. A clinicopathologic study of 238 cases. Cancer. 1992;69(12):2921–31.